Identification of XAF1 as an antagonist of XIAP anti-Caspase activity

Peter Liston*†, Wai Gin Fong†‡, N. Lynn Kelly§, Shingo Toji¶, Toshiaki Miyazaki¶, Damiano Conte‡, Katsuyuki Tamai, Constance G. Craig§, Michael W. McBurney* and Robert G. Korneluk‡§#

*Cancer Research Group, Ottawa Regional Cancer Center, 501 Smyth Road, Ottawa, K1H 8L6, Canada
‡Department of Biochemistry, Microbiology and Immunology, University of Ottawa, 401 Smyth Road, Ottawa, K1H 8L1, Canada
§Aegera Oncology Inc., 451 Smyth Road, Ottawa, K1H 8MS, Canada
¶Medical and Biological Laboratories Co., Naka-ku, Nagoya 460, Japan
†These authors contributed equally to this work
#e-mail: bob@mgcheo.med.uottawa.ca

The inhibitors of apoptosis (IAPs) suppress apoptosis through the inhibition of the caspase cascade and thus are key proteins in the control of cell death. Here we have isolated the protein XIAP-associated factor 1 (XAF1) on the basis of its ability to bind XIAP, a member of the IAP family. XIAP suppresses caspase activation and cell death *in vitro*, and XAF1 antagonizes these XIAP activities. Expression of XAF1 triggers a redistribution of XIAP from the cytosol to the nucleus. XAF1 is ubiquitously expressed in normal tissues, but is present at low or undetectable levels in many different cancer cell lines. Loss of control over apoptotic signalling is now recognized as a critical event in the development of cancer. Our results indicate that XAF1 may be important in mediating the apoptosis resistance of cancer cells.

The inhibitor of apoptosis (IAP) gene family encode proteins that have emerged as key, intrinisic inhibitors of the caspase cascade, and thus represent critical regulatory factors in apoptosis signalling. X-linked inhibitor of apoptosis (XIAP; also known as MIHA, ILP) is a particularly potent member of this family, which includes human IAP1 (HIAP1; cIAP2, MIHB), HIAP2 (cIAP1, MIHC), NAIP and Survivin[1–6]. A protein is included in this family if it possesses one or more baculovirus IAP repeats (BIR), a characteristic cysteine-rich domain of about 80 amino acids.

XIAP possesses three BIR domains and a carboxy-terminal RING zinc-finger. The BIR domains of XIAP, HIAP1, and HIAP2 have been shown to bind and inhibit caspase-3, -7 and -9 (refs 7–10). The smallest member of the IAP gene family, Survivin, contains only a single BIR, and also inhibits caspase-3 (refs 11, 12).

Despite the sequence similarity between the BIR domains of XIAP, they exhibit different affinities in terms of binding and inhibiting caspases[10]. Furthermore, it has been shown that XIAP can be cleaved by activated caspases *in vitro* and in Fas-stimulated cells into BIR1-2 and BIR3-RING zinc-finger fragments[13]. The amino-terminal BIR1-2 fragment is specific for caspases-3 and -7, but does not appear to be stable in Fas-treated cells. In contrast, the BIR3 RING fragment accumulates in Fas-treated cells, and specifically inhibits caspase-9. Exogenous expression of the BIR3 RING fragment potently suppresses Bax-induced apoptosis, a pathway that proceeds through the release of cytochrome *c*, the activation of Apaf-1 and the subsequent recruitment of caspase-9 (ref. 13).

The RING fingers of XIAP and HIAP2 possess E3 ubiquitin ligase activity, and appear to be responsible for self-degradation of these IAPs through the proteosome, in response to certain apoptotic stimuli[14]. These results suggested that IAP accumulation is self-regulated, a finding that was supported by the observation that deletion of the XIAP RING finger resulted in higher levels of protein accumulation and better protection from etoposide-induced apoptosis. The RING finger may not only function as negative regulator of the IAPs, however, as the RING finger of HIAP1 mediates the ubiquitination of caspases-3 and -7 (ref. 15). These experiments suggest that the IAPs initially bind and inhibit caspases, and subsequently ubiquitinate and trigger the proteolysis of the IAP–caspase complex.

The RING zinc-finger of XIAP can also mediate an interaction with bone morphogenic protein receptor-1A, with the BIR region subsequently recruiting TAB1/TAK1 complexes to the receptor[16]. In this context, it appears that XIAP functions as an adapter molecule necessary for morphogenic signalling. It has also been shown that XIAP can activate nuclear factor kappa B (NF-κB) through the activation of TAK1 (ref. 17). Whether these activities are independent the anti-caspase and E3 ubiquitin ligase activities of XIAP remain to be determined.

Despite overall simiarities in protein structure and biochemical function, each of the IAPs display unique protein–protein interactions implicating them in distinct signalling pathways. To identify XIAP protein interactions, here we have isolated a previously uncharacterized protein that we termed XAF1 (for XIAP-associated factor 1). XAF1 is a nuclear protein that directly interacts with endogenous XIAP and results in XIAP sequestration in nuclear inclusions. *In vitro* assays show that XAF1 antagonizes the anti-caspase activity of recombinant XIAP and reverses the protective effect of XIAP overexpression in cell lines. Notably, XAF1 either is not expressed or is present in only low levels in most cancer cell lines. Antisense induced depletion of XAF1 results in increased resistance to etoposide-triggered cell death, illustrating the survival advantage that cancer cells may attain by downregulation of XAF1.

Results

Isolation of a XIAP-interacting protein. We used the yeast two-hybrid method to identify cellular proteins that interact with XIAP. Full-length XIAP protein was expressed in yeast using the bait plasmid pAS2. A human placental complementary DNA library was screened and 24 interacting clones were selected for further characterization. Seven non-identical positive clones were obtained which encoded part or all of a protein that we termed XAF1 (GenBank accession no. X99699). The protein encoded by the open reading frame (ORF) is predicted to contain 301 amino acids and has the potential to form seven zinc-fingers. No other domain structures are immediately obvious. Searching of the NIH protein database using the GCG Blast program (http://www.gcg.com) revealed that the N-terminal five zinc-fingers of XAF1 share 41 and 22% amino-acid

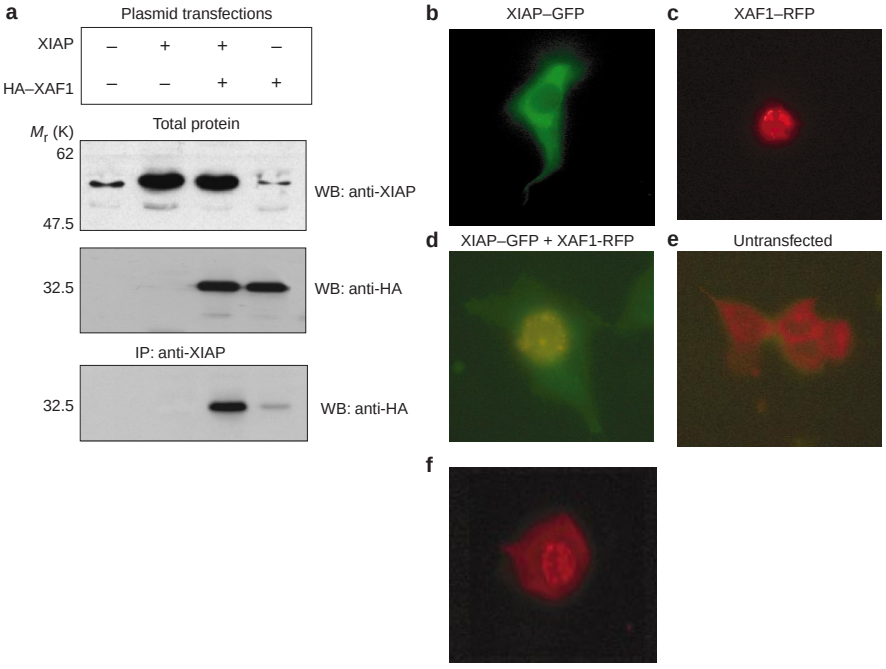

Figure 1 **Interaction analysis of XIAP and XAF1. a**, Confirmation of yeast two-hybrid identification of XIAP–XAF1 interaction by immunoprecipitation. HeLa cells were transiently transfected with the indicated plasmids for 48 h. Cell extracts were analysed by western blot (WB) using rabbit polyclonal anti-XIAP or monoclonal anti-HA antibody. Immunoprecipitation (IP) using anti-XIAP antibody, followed by WB with anti-HA confirmed the *in vivo* interaction of XIAP and XAF1. Molecular weight markers are indicated on the left. **b**, **c**, Subcellular localization of XIAP and XAF1 proteins. XIAP protein was expressed as a C-terminal fusion to GFP (**b**) and XAF1 was expressed as a fusion with RFP (**c**) in HeLa cells, and visualized under ultraviolet illumination. **d**, Co-expression of XIAP and XAF1 results in a redistribution of XIAP. HeLa cells were transfected using XIAP–GFP and XAF1–RFP expression plasmids, and visualized as in **b**, **c**. Areas of colocalization are indicated by the yellow/orange fluorescence. **e**, Localization of endogenous XIAP protein. HeLa cells were stained using anti-XIAP polyclonal antibody and a goat anti-rabbit-Cy3 conjugated antibody to visualize the cellular distribution of XIAP protein in normal (untransfected) cells. **f**, XAF1 expression triggers a redistribution of endogenous XIAP protein. HeLa cells were transfected with the plasmid pCI-XAF1 and stained using anti-XIAP polyclonal antibody and a goat anti-rabbit-Cy3 conjugated antibody to visualize the cellular distribution of XIAP. Expression of XAF1 resulted in pronounced nuclear staining.

identity with the zinc-finger domains of FLN 29 and tumour-necrosis factor-α receptor-associated factor 6 (TRAF6), respectively. FLN 29 has been entered into the database as a TRAF-interacting protein, but no information is currently available regarding its function.

We confirmed the interaction between XIAP and XAF1 *in vitro* by using immobilized gluthathione *S*-transferase (GST)–XIAP on a glutathione-agarose affinity column, as well as by immunoprecipitation analysis. Plasmids encoding XIAP and haemagglutinin A (HA)-tagged XAF1 protein were transfected into HeLa cells alone or in combination, and protein expression was confirmed by western blot analysis of whole-cell lysates (Fig. 1a). Immunoprecipitation of overexpressed XIAP protein with anti-XIAP polyclonal antibody co-precipitated XAF1, as detected by western blot of the precipitates with anti-HA antibody. A lesser quantity of XAF1 protein was also precipitated in cells that expressed only endogenous levels of XIAP protein (Fig. 1a). The subcellular localization of XIAP and XAF1 was investigated using green (GFP) and red (RFP) fluorescent protein tags fused to the C terminus of XIAP and XAF1, respectively (Clontech Living Colors vectors). XIAP–GFP localized to the cytoplasm, with an accentuation in the peri-nuclear region (Fig. 1b). In contrast, XAF1–RFP was located exclusively in the nucleus, often appearing to line the nuclear envelope and displaying distinct inclusions of variable size and number (Fig. 1c).

Given the discrete partitioning of these two proteins, we next determined whether co-expression would alter the cellular location of one or both fusion proteins. As seen in Fig. 1d, expression of RFP–XAF1 resulted in the redistribution of GFP–XIAP to the nucleus, as determined by the yellow stain. The redistribution of endogenous XIAP protein was confirmed using immunofluorescence microscopy. As seen in Fig. 1e, the endogenous XIAP protein was observed in the cytoplasm. Expression of the XAF1 protein (Fig. 1f) triggered a redistribution of most of the endogenous XIAP protein to the nucleus.

XAF1 inhibits the anti-caspase activity of XIAP *in vitro*. As XAF1 protein interacted with XIAP, we thought that XAF1 may antagonize the anti-apoptotic activity of XIAP, either by sequestering XIAP or by directly inhibiting the known anti-caspase activity of XIAP. We used a colorimetric assay (ApoAlert, Clontech) to monitor caspase-3 activity in the presence of recombinant, bacterially expressed GST fusion proteins. The addition of GST–XIAP (125 nM) reduced the rate of DEVD-pNA hydrolysis to roughly 5% of that of the control reaction containing caspase-3 and GST. GST–XAF1 was found to reverse the XIAP-mediated inhibition of caspase-3. The presence of 40 nM, 125 nM and 375 nM GST–XAF1 (1:3, 1:1 and 3:1 ratios of GST–XAF1:GST–XIAP) resulted in 12%, 49% and 82% of the activity of the control caspase-3/GST reaction, respectively (Fig. 2a). The total protein content of each reaction was kept constant through the addition of GST.

To extend these results to cellular model systems, we generated recombinant adenoviruses encoding XIAP and XAF1 expressed from the chicken β-actin promoter. We and others have previously established that overexpression of XIAP can suppress apoptosis triggered by many physiological and chemical triggers, including serum withdrawal and etoposide exposure[5,7,9]. We therefore sought to determine whether the presence of XAF1 would interfere with XIAP-mediated protection in these established paradigms.

HEL 299 fibroblast cells were doubly infected with adeno-*xiap* and either adeno-*lacZ* or adeno-*xaf1*. After allowing expression of

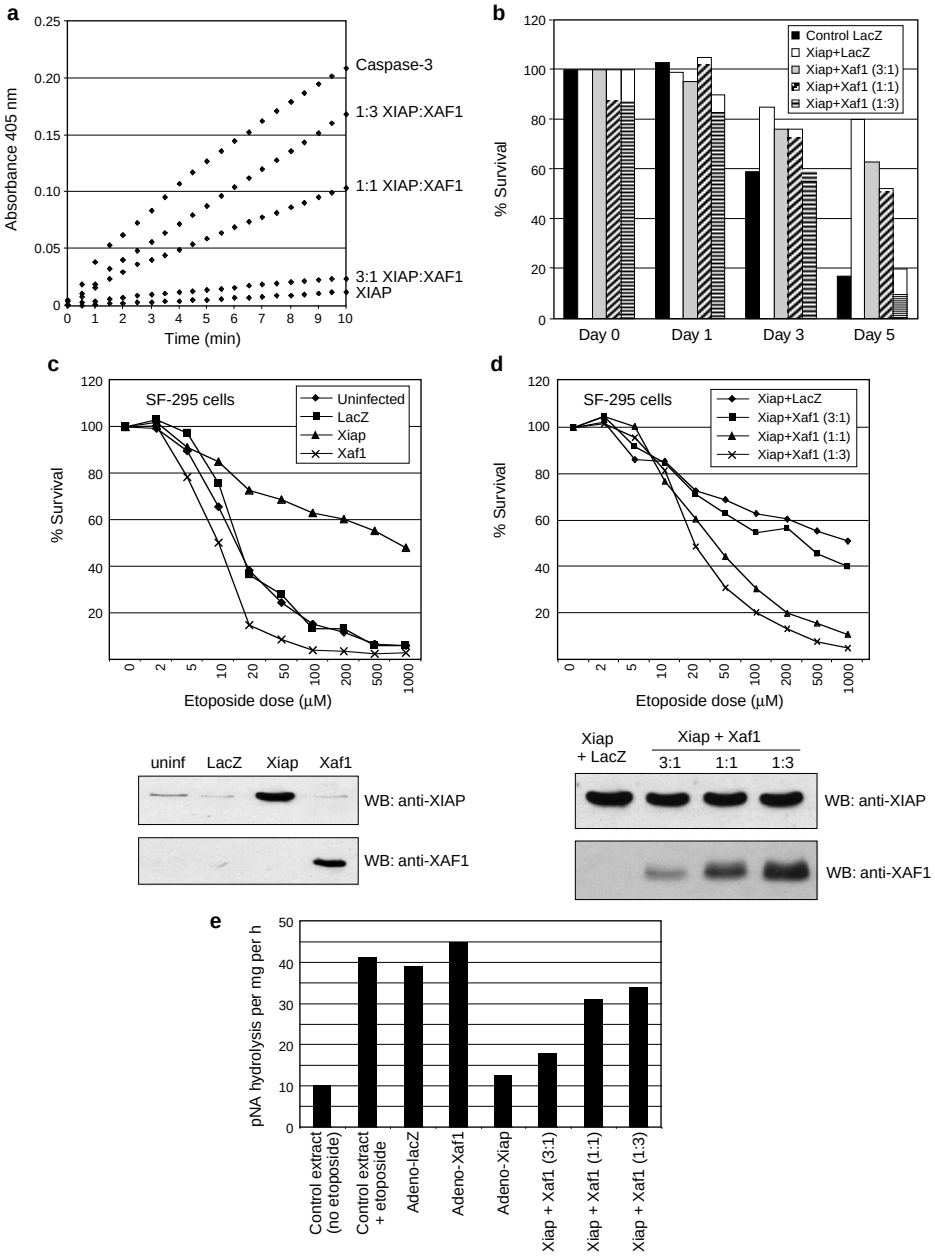

Figure 2 **XAF1 antagonizes XIAP–caspase interaction. a**, *In vitro* Capase-3 reactions were monitored at 30-s intervals using the DEVD-pNA chromophore. The addition of excess GST–XIAP inhibits more than 90% of this activity, but is reversed by increasing ratios of GST–XAF1 (see Methods). **b**, Adeno-*xiap* confers protection against serum withdrawal in HEL 299 cells, which is reversed by co-infection with adeno-*xaf1*. Control LacZ cells were infected at an MOI of 20 (see Methods). **c**, Adeno-*xiap* protects SF-295 cells, while adeno-*xaf1* increases sensitivity to etoposide triggered apoptosis. Cells were infected with adeno-*lacZ* (MOI = 10), adeno-*xiap* + adeno-*LacZ* (MOI = 5 each) or adeno-*xaf1* + adeno-*lacZ* (MOI = 5 each). After 24 h, the cells were exposed to etoposide for 4 h, and viability was determined 18 h later by WST-1 assay. **d**, Co-infection with adeno-*xaf1* reverses adeno-*xiap*-mediated protection from etoposide-induced apoptosis. SF-295 cells were infected with recombinant adenoviruses (see Methods). **f**, caspase-3-like activity present in extracts prepared from SF-295 cells infected as in **c**. Extracts were prepared 8 h after etoposide exposure (100 mM). Overexpression of XIAP significantly reduced rates of DEVD-pNA hydrolysis. Overexpression of XAF1 along with XIAP partially or completely restored caspase-3-like activity. Extracts prepared from uninfected cells, but not exposed to etoposide, are included to indicate basal levels of caspase-3-like activity in extracts prepared from non-apoptotic cells.

the recombinant proteins for 24 h, cells were washed with PBS and incubated in serum-free media. Viable cell counts were determined by trypan blue exclusion at 1, 3 and 5 days after serum withdrawal. Adeno-*xiap* infection resulted in significant protection relative to control adeno-*lacZ* infected cells (80% compared with 17% survival at day five). Co-infection of adeno-*xiap*-infected cells with increasing ratios of adeno-*xaf1* resulted in a dose-dependent reversal of protection. Adeno-*xaf1*:adeno-*xiap* co-infection ratios of 1:3, 1:1 and 3:1 reduced the 5-day survival levels from 80% to 63%, 52% and 20%, respectively (Fig. 2b).

We next examined whether XAF1 could block the ability of XIAP to suppress etoposide-triggered apoptosis in SF-295 glioblastoma cells, which do not express endogenous XAF1. Cells were plated in 96-well plates and infected with combinations of adeno-*lacZ*,

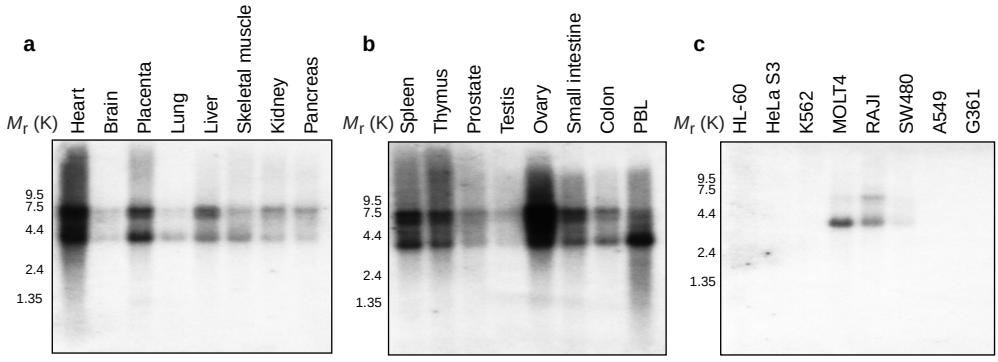

Figure 3 **Xaf1 is underexpressed in many cancer cell lines.** Northern blot analysis showing ubiquitous expression of *xaf1* in normal tissues and cells (**a**, **b**), with low or absent expression in cancer cell lines (**c**). PBL, peripheral-blood leukocyte.

adeno-*xiap* or adeno-*xaf1*. At 24 h after infection, triplicate samples were exposed to etoposide in doses ranging from 2 mM to 1 mM for 4 h, and then incubated in normal media for 18 h. Cell viability was determined using WST-1 reagent (Boerhinger-Mannheim). As shown in Fig. 2c, adeno-*xiap* gave significant protection across the entire etoposide dose range as compared with uninfected or adeno-*lacZ* infected cells. In contrast, infection with adeno-*xaf1* triggered increased sensitivity to etoposide-mediated killing, but did not appear to be capable of initiating apoptotic cell death in isolation.

Co-infection of adeno-*xiap* and adeno-*xaf1* resulted in a partial to total reversal of XIAP-mediated protection in a dose-dependent manner, similar to that observed in the serum-withdrawal experiments (Fig. 2d). Western blot analysis showed that increasing the amount of co-infecting adeno-*xaf1* did not decrease the transducing efficiency of the adeno-*xiap* virus. To confirm that these effects were mediated by modulation of caspase activity, protein lysates were prepared from cells infected with the recombinant adenoviruses 8 h after exposure to 100 mM etoposide, at which time caspase-3 activity is maximal (data not shown).

Extracts were analysed for caspase-3-like activity by measuring the rate of DEVD-pNA hydrolysis per mg of total protein. Infection with adeno-*xaf1* resulted in a marginal increase in caspase-3-like activity that was not statistically significant (Fig. 2e). In contrast, overexpression of XIAP protein suppressed about 70% of the caspase-3-like activity present in extracts of uninfected cells or cells infected with adeno-*lacZ* alone. In agreement with the survival assays, extracts prepared from cells co-infected with adeno-*xiap* + adeno-*xaf1* in increasing ratios (3:1, 1:1 and 1:3 XIAP:XAF1) resulted in partial reversion, with levels of caspase-3-like activity rising to about 90% of control adeno-*lacZ*-infected extracts (Fig. 2e).

Xaf1 messenger RNA is underexpressed in most cancer cell lines. As XAF1 could antagonize the anti-apoptotic properties of XIAP, we next examined the distribution of *xaf1* mRNA expression in both normal tissues and transformed cell lines. Expression analysis was performed by hybridizing multitissue poly(A)$^+$ northern blots (Clontech) with a probe derived from the N-terminal 750 base pairs (bp) of the XAF1 ORF.

Expression is widespread with mRNA levels highest in heart and ovary and lowest in brain and testis (Fig. 3). At least four distinct transcript sizes were observed, at about 3.9 kilobases (kb), 4.5 kb, 6.0 kb and 7.0 kb. Preliminary characterization of additional clones isolated from a human liver complementary DNA library strongly suggests that alternative splicing is the source of the transcript variants (W.G.F. and R.G.K., unpublished data). Southern blot analysis indicates that only a single copy of the *xaf1* gene exists in the genome[18].

Notably, five of the eight cancer cell lines tested exhibited undetectable levels of *xaf1* mRNA. Furthermore, in those cell lines that did express *xaf1*, the 3.9-kb transcript predominated (Fig. 3c). We have extended these observations to the 60-cell-line panel of the National Cancer Institute. Using real-time quantitative polymerase chain reaction (PCR), all these cell lines were found to express little or no *xaf1* mRNA; and 37 (62%) of the cell lines expressed less than 1% of the *xaf1* mRNA levels found in normal liver[18]. Notably, the *xaf1* gene has been mapped distal to *TP53* on chromosome 17—a region known to be associated with loss of heterozygosity [18]. However, Southern blot analysis provided no indication of gross rearrangements or deletion of both copies of the *xaf1* gene in all cancer cell lines tested (data not shown). The basis for the reduced expression of *xaf1* mRNA in cancer cell lines remains to be resolved.

Reduced expression of XAF1 enhances resistance to apoptosis. To determine whether the loss of endogenous *xaf1* expression enhances cellular resistance to apoptosis, we generated an antisense *xaf1* adenovirus and used this to infect cell lines that have relatively high (SF-539, OVCAR-5) or low to undetectable (SF-295, OVCAR-3) levels of *xaf1* mRNA. Western blot analysis using a polyclonal antibody raised against GST–XAF1 revealed a reactive protein, with a relative molecular mass of about 34,000 (M_r 34K), in SF-539 and OVCAR-5 cell extracts that was not evident in either the SF-295 or OVCAR-3 extracts (Fig. 4a). Infection of SF-539 cells with the antisense *xaf1* adenovirus (adeno-*xafas*, multiplicity of infection (MOI) = 10) reduced the intensity of this protein band in a time-dependent manner (Fig. 3b).

We next determined the effect of the antisense *xaf1* adenovirus on etoposide-induced killing of SF-295 and SF-539 cells. Cells were infected with either adeno-*xafas* or control adenoviruses, and etoposide was added 24 h after infection for 4 h. Analysis of SF-539 cell survival 18 h later revealed that the adeno-*xafas* adenovirus conferred significant protection at intermediate etoposide exposures, but that this effect diminished at higher doses of etoposide (Fig. 4c).

In contrast, adeno-*xafas* had no effect in the SF-295 cell line, which expresses very little *xaf1* mRNA (Fig. 4d). In a similar manner, adeno-*xafas* infection of OVCAR-5 decreased the sensitivity of these cells to etoposide (Fig. 4e). The magnitude of the antisense effect was diminished in OVCAR-5 relative to that in SF-295 cells, presumably because of lower expression levels of endogenous XAF1 protein and higher levels of XIAP protein (Fig. 4a). Analysis of OVCAR-3 cells, which do not express detectable levels of *xaf1* mRNA, also showed no effect of the antisense *xaf1* virus (data not shown).

These results were further reinforced with analysis of caspase-3-like activity in cell extracts prepared from cells exposed to 100 μM etoposide for 8 h. As seen in Fig. 4f, infection with adeno-*xafas* suppressed caspase-3-like activity in extracts prepared from SF-539 and OVCAR-5 cells, albeit to a lesser extent that adeno-*xiap* infection. In contrast, adeno-*xafas* had no effect on caspase-3-like activity in SF-295 cells.

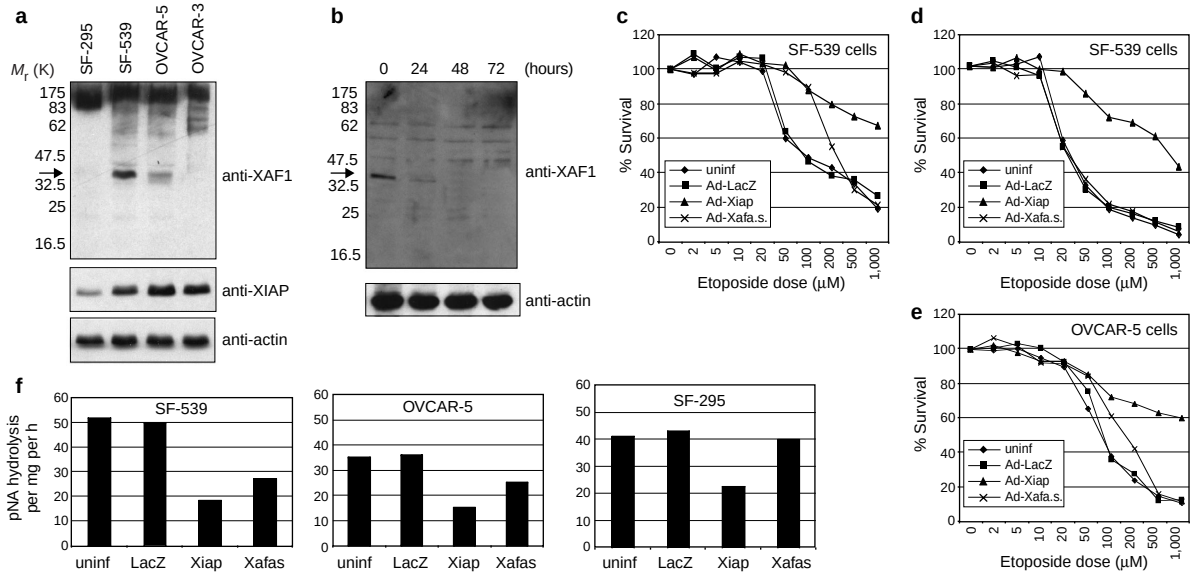

Figure 4 **Abolishing XAF1 protein increases apoptotic resistance in cell lines that retain endogenous expression. a**, Rabbit anti-XAF1 antibody detects a ~34K protein (arrow) in SF-539 and OVCAR-5 cells, but not in SF-295 or OVCAR-3 cells. Endogenous XIAP protein levels were significantly lower in SF-295 cells relative to other cell lines. **b**, Downregulation of endogenous XAF1 protein (arrow) by antisense adeno-*xaf1* (adeno-xafas). SF-539 cells were infected with adeno-*xafas*, expressing the *xaf1* ORF in the reverse orientation (antisense *xaf1*, MOI = 10), and collected 0, 24, 48 and 72 h after infection. In **a** and **b**, actin levels were determined to control for protein loading. **c**, Adeno-*xafas* suppresses apoptosis of SF-539 cells at intermediate etoposide exposure levels. Cultures of SF-539 cells were infected with the indicated adenoviruses and exposed to etoposide. **d**, Adeno-*xafas* does not protect SF-295 cells, which express low levels of endogenous XAF1 protein. Cultures of SF-295 cells were infected with the indicated adenoviruses and exposed to etoposide. **e**, Adeno-*xafas* also suppresses apoptosis of OVCAR-5 cells at intermediate etoposide exposure levels. OVCAR-5 cells, treated as in **c**, show that downregulation of XAF1 increases resistance to etoposide killing at intermediate dosages. Both the levels of endogenous XAF1 protein and the degree of protection mediated by antisense *xaf1* are reduced compared with in SF-539 cells. **f**, caspase-3-like activity is decreased in both SF-539 and OVCAR-5 cells infected with the antisense *xaf1* adenovirus. caspase-3-like activity was measured by DEVD-pNA hydrolysis in extracts from SF-539, OVCAR-5 and SF-295 cells infected with the recombinant adeno viruses (MOI = 5) and exposed to 100 μM etoposide for 8 h. Adeno-*xafas* diminished levels of caspase-3-like activity, albeit to a lesser extent than adeno-*xiap*. This effect was evident only in cell lines expressing endogenous XAF1 (SF-539, OVCAR-5), and not in SF-295 cells, which express undetectable levels of XAF1 protein.

Discussion

The initiation of the self-amplifying caspase cascade was considered by many to be the 'point of no return', after which the cell was irrevocably committed to apoptosis. We now know that limited activation of caspases can be controlled, and may in fact be required for some normal cellular processes, such as T-cell activation[19,20]. The IAP proteins are the only endogenous inhibitors of the terminal or effector caspases identified to date, and provide a mechanism for limiting or halting the cascade. Although HIAP1 and HIAP2 have been identified as components of the TNF receptor complex[2,21], little is known regarding the signal transduction pathways in which XIAP functions. We therefore screened a yeast two-hybrid library and isolated a zinc-finger protein that interacts with XIAP, which we termed XAF1 (for XIAP associated factor 1).

Biochemical assays using purified, recombinant proteins revealed that XAF1 directly inhibited the anti-caspase activity of XIAP. Consistent with this, we observed that XAF1 overexpression reversed XIAP-mediated protection against apoptosis. Subcellular distribution studies revealed that XAF1 resides in the nucleus, and can effect a marked relocalization of either endogenous or overexpressed XIAP protein from the cytoplasm to the nucleus. Both the biochemical neutralization and the sequestering of XIAP in nuclear inclusions are compatible with the observed increase in the sensitivity of some cell lines to apoptotic triggers when XAF1 is overexpressed.

This model suggests that XAF1 functions as a negative regulator of the IAPs, analogous to the situation in *Drosophila*. Cell death in insects appears to be regulated predominantly by the balance of IAPs and caspases, with the pro-apoptotic proteins Reaper, HID and Grim capable of triggering apoptosis by antagonizing the anti-caspase activity of D-IAP1 and D-IAP2 (refs 22–24).

No mammalian homologues of HID, Reaper or Grim have been identified to date; however, both XAF1 and the DIABLO/Smac protein functionally resemble these proteins by sequestering or inhibiting the activity of cellular IAP proteins[25,26]. In contrast to the insect proteins, overexpression of either XAF1 or DIABLO/Smac does not appear to induce apoptosis, but does sensitize cells to additional cell death triggers. DIABLO/Smac is a mitochondrial protein that is released into the cytoplasm in response to apoptotic triggers, whereupon it neutralizes the inhibitory activity of the IAPs[25,26]. In contrast, XAF1 does not require an activation signal, and appears to constitutively interact with XIAP and inhibit its function in healthy cells.

The decreased expression of *xaf1* that we observed in several cancer cell lines suggests that alterations in the balance of IAP and caspase activities is a common occurrence in the development of the transformed state. There are obvious survival benefits to cells that either upregulate IAPs or downregulate their inhibitors, as observed for XAF1. Overexpression of the IAPs has been reported to protect cells from irradiation and compounds used in chemotherapy numerous times. Here we used an antisense expression vector to show that loss of XAF1 expression can also enhance resistance to apoptosis in cell lines that express appreciable levels of the protein. Intriguingly, the *xaf1* gene is located in a chromosomal region associated with loss of heterozygosity, underscoring the importance of resolving the basis for the loss of *xaf1* expression in cancer cells. □

Methods

Yeast two-hybrid analysis.

The plasmid pAS2–XIAP was constructed by inserting the full-length coding region of XIAP in-frame with the GAL4 DNA-binding domain. This construct and a human placental cDNA library in the vector pACT (Clontech) were co-transfected into yeast strain Y187 and HIS^+, $LacZ^+$ clones were selected.

Plasmid constructs and fluorescence imaging.

The HA-tagged Xaf1 ORF and 3' untranslated region were subcloned from pACT into pCI (Promega) using standard techniques. The XAF1 ORF was also PCR amplified with primers that deleted the stop codon for insertion into the plasmid DsRED-N1 (Clontech). The XIAP ORF was amplified in a similar manner for insertion into the plasmid eGFP–N1 (Clontech). Imaging was performed on a Zeiss Axiophot fluorescence microscope using a Sony 3CCD PowerHAD camera and Northern Eclipse version 5.0 software.

Immunofluorescent visualization of endogenous XIAP protein was performed by fixing cells in 1% glutaraldehyde/1 x PBS/1% Triton X-100. Slides were washed in PBS and stained with rabbit anti-XIAP polyclonal antisera diluted 1:200 in PBS. After washing, antibody complexes were visualized with goat anti-rabbit Cy3 conjugated antibody (1:200 dilution, Amersham) under a Zeiss Axiophot fluorescence microscope.

Preparation of antibodies.

Polyclonal anti-XAF1 antibody was generated by immunizing rabbits with GST–XAF1 fusion protein in RIBI adjuvant (Sigma). Antiserum was cleared of anti-GST antibody on a GST–agarose column then positively selected on a GST–XAF1-agarose column.

Immunoprecipitation analysis.

Protein extracts were prepared from cells 48 h after transfection (Lipofectamine Plus, GibcoBRL) in lysis buffer containing 10% Triton X-100, 10% glycerol, 400 mM NaCl, 10 mM Tris pH 8.0, 1 mM phenyl methyl sulphonyl fluoride and 10 mg ml^{-1} aprotinin. Lysates were pre-cleared with 10 ml of rabbit pre-immune serum coupled to protein A sepharose for 2 h, followed by low-speed centrifugation. Immunoprecipitations were performed using 5 mg of affinity-purified rabbit polyclonal anti-XIAP antibody for 2 h. Protein A-Sepharose was added for 1 h, and antibody complexes were collected and washed five times in lysis buffer. Proteins were eluted in low pH glycine buffer (pH 3.5, 50 mM), and resolved on 12.5% SDS–PAGE gels followed by electrophoretic transfer to PVDF membranes (Immobilon). Western blot analysis was carried out using monoclonal anti-HA (Boehringer-Mannheim) with an anti-mouse secondary antibody coupled to horse radish peroxidase (Amersham). Proteins were visualized by electrochemiluminscence (Amersham).

Northern blot analysis.

Human multiple-tissue northern blots (Clontech MTN blot I, blot II and cancer cell line blot I) containing 2 mg $poly(A)^+$ mRNA were probed with a [^{32}P]dCTP-labelled (Amersham), random-primed (Amersham Rediprime) DNA probe spanning the first 750 nucleotides of the *xaf1* ORF. Blots were hybridized, washed and exposed to X-ray film concurrently, according to the manufacturer's instructions.

caspase-3 inhibition assays.

GST–XIAP and GST–XAF1 were prepared by two-step purification on glutathione-agarose beads (Pharmacia) followed by affinity purification on immobilized monoclonal anti-XIAP or anti-XAF1 antibody columns. Recombinant human caspase-3 was expressed in *Escherichia coli* using the pET-28a(+) expression system (Novagen) and purified on a nickel-NTA-agarose affinity column (Qiagen). caspase-3 activity was measured using *p*-nitroanilide conjugated DEVD peptide substrate (ApoAlert, Clontech). DEVD-pNA hydrolysis was monitored at 30-s intervals using a spectrophotometer. In Fig. 2a, the following combinations of GST–XIAP and GST–XAF1 were used: 'XIAP' = 125 nM GST–XIAP protein + 375 nM GST; '3:1 XIAP:XAF1' = 125 nM GST–XIAP protein + 40 nM GST–XAF1 protein + 335 nM GST (total protein 500 nM); '1:1 XIAP:XAF1' = 125 nM GST–XIAP protein + 125 nM GST–XAF1 protein + 250 nM GST (total protein 500 nM); '1:3 XIAP:XAF1' = 125 nM GST–XIAP protein + 375 nM GST–XAF1 protein (total protein 500 nM). 'caspase-3' = control reaction containing 500 nM GST.

Recombinant adenovirus.

Recombinant adeno-*xaf1* and the antisense *xafas* vectors were constructed by blunt-end ligation of the *xaf1* coding region into the Swa 1 site of the cosmid pAdex1CA. The cosmids were co-transfected into 293 cells with Ad5dlX–TPC complex, and recombinant viruses were plaque purified. Vectors and protocols have been described[27], as has the construction of adeno-*lacZ* and adeno-*xiap*[28,29].

Survival assays.

Serum withdrawal assays were performed on HEL 299 cells plated in triplicate on 24-well dishes in DMEM/ 10% fetal calf serum (FCS). Cells were infected with recombinant adenoviruses at the indicated MOIs for 24 h, and washed twice with PBS before serum-free DMEM was added. Cell viability was determined by trypan-blue exclusion as described[4]. Etoposide kill curves were performed in 96-well dishes containing 3,000 cells per well in MEM/ 10% FCS. Cells were infected with the recombinant adenoviruses at an MOI of 5 unless otherwise stated. In Fig. 2b, the following combinations of adenoviruses were used: 'XIAP + LacZ' = infection with adeno-*xiap* (MOI of 10) + adeno-*LacZ* (MOI of 10); 'XIAP + XAF1(1:3)' = infection with adeno-*xiap* (MOI of 10) + adeno-*xaf1* (MOI of 3); 'XIAP + XAF1(1:1)' = infection with adeno-*xiap* (MOI of 10) + adeno-*xaf1* (MOI of 10); 'XIAP + XAF1(3:1)' = infection with adeno-*xiap* (MOI of 10) + adeno-*xaf1* (MOI of 30). In Fig. 2d, the following combinations of adenoviruses were used: 'XIAP + XAF1(1:3)' = infection with adeno-*xiap* (MOI of 5) + adeno-*xaf1* (MOI of 1.5); 'XIAP + XAF1(1:1)' = infection with adeno-*xiap* (MOI of 5) + adeno-*xaf1* (MOI of 5); 'XIAP + XAF1(3:1)' = infection with adeno-*xiap* (MOI of 5) + adeno-*xaf1* (MOI of 15).

Twenty-four hours after infection, etoposide was added for 4 h. The media was then replaced, and cell viability determined 18 h later using the WST-1 reagent according to the manufacturer's instructions (Boehringer-Mannheim).

RECEIVED 31 MAY 2000; REVISED 24 JULY 2000; ACCEPTED 27 SEPTEMBER 2000;
PUBLISHED 10 JANUARY 2001.

1. Roy, N. *et al.* The gene for neuronal apoptosis inhibitory protein is partially deleted in individuals with spinal muscular atrophy. *Cell* **80,** 167–178 (1995).
2. Rothe, M., Pan, M., Henzel, W. L.., Ayres, T. M. & Goeddel, D. V. The TNFR2-TRAF signaling complex contains two novel proteins related to baculoviral inhibitor of apoptosis proteins. *Cell* **83,** 1243–1252 (1995).
3. Liston, P. *et al.* Suppression of apoptosis in mammalian cells by NAIP and a related family of IAP genes. *Nature* **379,** 349–353 (1996).
4. Duckett, C. S. *et al.* A conserved family of cellular genes related to the baculovirus iap gene and encoding apoptosis inhibitors. *EMBO J.* **15,** 2685–2694 (1996).
5. Uren, A. G., Pakusch, M., Hawkins, C. J., Puls, K. L. & Vaux, D. L. Cloning and expression of apoptosis inhibitory protein homologues that function to inhibit apoptosis and/or bind tumor necrosis factor receptor-associated factors. *Proc. Natl Acad. Sci. USA* **93,** 4974–4978 (1996).
6. Ambrosini, G., Adida, C. & Altieri, D.C. A novel anti-apoptosis gene, survivin, expressed in cancer and lymphoma. *Nature Med.* **3,** 917-921 (1997).
7. Deveraux, Q. L., Takahashi, R., Salvesen, G. S. & Reed, J. C. X-linked IAP is a direct inhibitor of cell death proteases. *Nature* **388,** 300–304 (1997).
8. Roy, N., Deveraux, Q. L., Takahashi, R., Salvesen, G. S. & Reed, J. C. The c-IAP-1 and c-IAP-2 proteins are direct inhibitors of specific caspases. *EMBO J.* **16,** 6914–6925 (1997).
9. Deveraux, Q. L. *et al.* IAPs block apoptotic events induced by caspase-8 and cytochrome c by direct inhibition of distinct caspases. *EMBO J.* **17,** 2215–2223 (1998).
10. Takahashi, R. *et al.* A single BIR domain of XIAP sufficient for inhibiting caspases. *J. Biol. Chem.* **273,** 7787–7790 (1998).
11. Kobayashi, K., Hatano, M., Otaki, M., Ogasawara, T. & Tokuhisa, T. Expression of a murine homologue of the inhibitor of apoptosis protein is related to cell proliferation. *Proc. Natl Acad. Sci. USA* **96,** 1457–1462 (1999).
12. Tamm, I. *et al.* IAP-family protein survivin inhibits caspase activity and apoptosis induced by Fas (CD95), Bax, caspases, and anticancer drugs. *Cancer Res.* **58,** 5315–5320 (1998).
13. Deveraux, Q. L. *et al.* Cleavage of human inhibitor of apoptosis protein XIAP results in fragments with distinct specificities for caspases. *EMBO J.* **18,** 5242–5251 (1999).
14. Yang, Y., Fang, S., Jensen, J.P., Weissman, A. M. & Ashwell, J. D. Ubiquitin protein ligase activity of IAPs and their degradation in proteosomes in response to apoptotic stimuli. *Science* **288,** 874–877 (2000).
15. Huang, H.-K. *et al.* The inhibitor of apoptosis, cIAP**2,** functions as a ubiquitin-protein ligase and promotes *in vitro* monoubiquitination of caspases 3 and 7. *J. Biol. Sci.* **275,** 26661–26664 (2000).
16. Yamaguchi, K. *et al.* XIAP, a cellular member of the inhibitor of apoptosis protein family, links the receptors to TAB1-TAK1 in the BMP signaling pathway. *EMBO J.* **18,**179–187.
17. Hofer-Warbinek, R. *et al.* Activation of NF-Kappa B by XIAP, the X chromosome-linked inhibitor of apoptosis, in endothelial cells involves TAK1. *J. Biol. Sci.* **275,** 22064–22068 (2000).
18. Fong, W. G. *et al.* Expression and genetic analysis of XIAP associated factor 1 (XAF1) in cancer cell lines. *Genomics* **70,** 113–122 (2000).
19. Alam, A., Cohen, L. Y., Aouad, S. & Sekaly, R. P. Early activation of caspases during T lymphocyte stimulation results in selective substrate cleavage in nonapoptotic cells. *J. Exp. Med.* **190,** 1879–1890 (1999).
20. Kennedy, N. J., Kataoka, T., Tschopp, J. & Budd, R. C. caspase activation is required for T cell proliferation. *J. Exp. Med.* **190,** 1891–1896 (1999).
21. Shu, H.-B., Takeuchi, M. & Goeddel, D. V. The tumor necrosis factor receptor 2 signal transducers TRAF2 and c-IAP1 are components of the tumor necrosis factor receptor 1 signaling complex. *Proc. Natl Acad. Sci. USA* **93,** 13973–13978 (1996).
22. Vucic, D., Kaiser, W. J. & Miller, L. K. Inhibitor of apoptosis proteins physically interact with and block apoptosis induced by *Drosophila* proteins HID and GRIM. *Mol. Cell Biol.* **18,** 3300–3309 (1998).
23. Goyal, L., McCall, K., Apapite, J., Hartwieg, E. & Steller, H. Induction of apoptosis by *Drosophila reaper, hid* and *grim* through inhibition of IAP function. *EMBO J.* **19,** 589–597 (2000).
24. Wang, S. L., Hawkins, C. J., Yoo, S. J., Muller, H. A. J. & Hay, B. A. The *Drosophila* caspase inhibitor DIAP1 is essential for cell survival and is negatively regulated by HID. *Cell* **98,** 453–463 (1999).
25. Du, C., Fang, M., Li, Y., Li, L. & Wang, X. Smac, a mitochondrial protein that promotes cytochrome c-dependent caspase activation by eliminating IAP inhibition. *Cell* **102,** 33–42 (2000).
26. Verhagen, A. M. *et al.* Identification of DIABLO, a mammalian protein that promotes apoptosis by binding to and antagonizing IAP proteins. *Cell* **102,** 43–53 (2000).
27. Miyake, S. *et al.* Efficient generation of recombinant adenoviruses using adenovirus DNA-terminal protein complex and a cosmid bearing the full-length virus genome. *Proc. Natl Acad. Sci. USA* **93,** 1320–1324 (1996).
28. Li, J. *et al.* Expression of inhibitor of apoptosis proteins (IAPs) in rat granulosa cells during ovarian follicular development and atresia. *Endocrinology* **139,** 1321–1328 (1998).
29. Xu, D. G. *et al.* Elevation of neuronal expression of NAIP reduces ischemic damage in the rat hippocampus. *Nature Med.* **3,** 997–1004 (1997).

ACKNOWLEDGEMENTS

We wish to thank the University of California San Francisco / Neurosurgery Tissue Bank for the SF-295 and SF-539 cell lines. P.L. is a Centennial Fellow of the Medical Research Council of Canada. This work was supported by grants to R.G.K. from the Networks of Centers of Excellence Canadian Genetic Diseases Network (CGDN), the Medical Research Council of Canada (MRC), and the Howard Hughes Medical Institute (HHMI). R.G.K. is a recipient of an MRC senior scientist award, a HHMI International Research Scholar, and a Fellow of the Royal Society of Canada. Correspondence and requests for materials should be addressed to R.G.K.

